

## Chiral sum rules and their phenomenology

John F. Donoghue and Eugene Golowich

*Department of Physics and Astronomy, University of Massachusetts, Amherst, Massachusetts 01003*

(Received 15 July 1993)

We present an analysis of four sum rules, each based on chiral symmetry and containing the difference  $\rho_V(s) - \rho_A(s)$  of isovector vector and axial-vector spectral functions. Experimental data from  $\tau$  lepton decay and electron-positron scattering identify the spectral functions over a limited kinematic domain. We summarize the status of the existing database. However, a successful determination of the sum rules requires additional content, in the form of theoretical input. We show how chiral symmetry and the operator product expansion can be used to constrain the spectral functions, respectively, in the low energy and the high energy limits and proceed to perform a phenomenological test of the sum rules.

PACS number(s): 11.55.Hx, 11.30.Rd, 13.10.+q

### I. MOTIVATION

Despite a concerted effort by physicists extending over many years, an understanding of QCD from first principles continues to be elusive. Fortunately, data continue to appear which provide a rather direct probe of the inner workings of the strong interactions.

A case in point involves semileptonic  $\tau$  lepton decay and hadron production in  $e^+e^-$  scattering. For both of these, multihadron states such as  $2\pi$ ,  $3\pi$ , . . . are excited from the operation of quark vector and axial-vector currents on the QCD vacuum. In this paper, we shall restrict our discussion to the isospin currents [1],

$$V_a^\mu = \bar{q} \frac{\tau_a}{2} \gamma^\mu q \quad \text{and} \quad A_a^\mu = \bar{q} \frac{\tau_a}{2} \gamma^\mu \gamma_5 q, \quad (1)$$

where  $a=1,2,3$  and  $q=(u,d)$ . Such current-induced processes provide information about the current bilinears,

$$\langle 0 | T(V_a^\mu(x) V_b^\nu(0)) | 0 \rangle$$

and (2)

$$\langle 0 | T(A_a^\mu(x) A_b^\nu(0)) | 0 \rangle.$$

It has been long recognized that these quantities appear in certain chiral sum rules. Since these sum rules follow rather directly from QCD and chiral symmetry, a test of their correctness is, in effect, an experimental check on the validity of QCD itself.

Unfortunately, there are several formidable obstacles to a successful implementation of this procedure. For one, the sum rules encompass an infinite range of energy, whereas existing data covers a very modest range,  $s < m_\tau^2$  for  $\tau$  decay and  $s \leq 5 \text{ GeV}^2$  in  $e^+e^-$  scattering. Moreover, as we shall see there are uncertainties in existing data which future experimental work must clear up.

We feel that such difficulties can be overcome. In this work, we shall argue that a combination of chiral symmetry and QCD sum rule methods constrain the low- and high-energy limits of the dispersion integrals and that data can be used to fill in much of the rest. The content of the paper is organized as follows. We begin by introducing the spectral functions and their sum rules in Sec. II, review the state of existing data in Sec. III, and then describe various theoretical constraints in Sec. IV. Armed with experimental data and theoretical constraints, we present details of a phenomenological analysis of the chiral sum rules in Sec. V. The final part in Sec. VI summarizes our findings.

### II. SPECTRAL REPRESENTATIONS

In this section, we shall work exclusively in the chiral world of massless  $u,d$  quarks. Here, the spin-0 axial contribution is given by the pion pole and the two-current time-ordered products can be expressed in terms of spin-1 spectral functions  $\rho_{V,A}(s)$  [2],

$$\langle 0 | T(V_a^\mu(x) V_b^\nu(0)) | 0 \rangle = i\delta_{ab} \int_0^\infty ds \rho_V(s) (-sg^{\mu\nu} - \partial^\mu \partial^\nu) \int \frac{d^4 p}{(2\pi)^4} \frac{e^{-ip \cdot x}}{p^2 - s + i\epsilon} \quad (3)$$

and

$$\langle 0 | T(A_a^\mu(x) A_b^\nu(0)) | 0 \rangle = -i\delta_{ab} F_\pi^2 \partial^\mu \partial^\nu \int \frac{d^4 p}{(2\pi)^4} \frac{e^{-ip \cdot x}}{p^2 + i\epsilon} + i\delta_{ab} \int_0^\infty ds \rho_A(s) (-sg^{\mu\nu} - \partial^\mu \partial^\nu) \frac{d^4 p}{(2\pi)^4} \frac{e^{-ip \cdot x}}{p^2 - s + i\epsilon}. \quad (4)$$

For completeness, we also give the corresponding relations involving non-time-ordered products,

$$\begin{aligned} \frac{1}{2\pi} \int d^4x e^{iq \cdot x} \langle 0 | V_a^\mu(x) V_b^\nu(0) | 0 \rangle &= i \delta_{ab} \rho_V(q^2) (q^\mu q^\nu - q^2 g^{\mu\nu}), \\ \frac{1}{2\pi} \int d^4x e^{iq \cdot x} \langle 0 | A_a^\mu(x) A_b^\nu(0) | 0 \rangle &= i \delta_{ab} [\rho_A(q^2) (q^\mu q^\nu - q^2 g^{\mu\nu}) + F_\pi^2 \delta(q^2) q^\mu q^\nu]. \end{aligned} \quad (5)$$

It follows from chiral symmetry and the high-energy behavior of QCD that the vector and axial-vector spectral functions contribute to certain sum rules [3],

$$\int_0^\infty ds \frac{\rho_V(s) - \rho_A(s)}{s} = -4\bar{L}_{10} = (2.73 \pm 0.12) \times 10^{-2}, \quad (6)$$

$$\int_0^\infty ds [\rho_V(s) - \rho_A(s)] = F_\pi^2 = (8.54 \pm 0.06) \times 10^{-3} \text{ GeV}^2, \quad (7)$$

$$\int_0^\infty ds s [\rho_V(s) - \rho_A(s)] = 0, \quad (8)$$

$$\begin{aligned} \int_0^\infty ds s \ln \left[ \frac{s}{\Lambda^2} \right] [\rho_V(s) - \rho_A(s)] \\ = -\frac{16\pi^2 F_\pi^2}{3e^2} (m_{\pi^\pm}^2 - m_{\pi^0}^2) \\ = -(6.19 \pm 0.03) \times 10^{-3} \text{ GeV}^4. \end{aligned} \quad (9)$$

In the remainder of the paper, we shall refer to the above sum rules, respectively, as  $W0$ ,  $W1$ ,  $W2$ , and  $W3$ . In the first one,  $W0$ , the quantity  $\bar{L}_{10}$  is related to the renormalized coefficient  $L_{10}^{(r)}(\mu)$  of an  $O(E^4)$  operator appearing in the effective chiral Lagrangian of QCD [4]. Although the value of  $L_{10}^{(r)}(\mu)$ , which is measured in the radiative pion decay  $\pi \rightarrow e\nu\gamma$ , refers to a renormalization scale  $\mu$ , the quantity  $\bar{L}_{10}$  is itself independent of  $\mu$ ,

$$\begin{aligned} \bar{L}_{10} &= L_{10}^{(r)}(\mu) + \frac{1}{192\pi^2} \left[ \ln \left[ \frac{m_\pi^2}{\mu^2} \right] + 1 \right] \\ &\simeq -(6.84 \pm 0.3) \times 10^{-3}. \end{aligned} \quad (10)$$

$$\frac{d\Gamma \left[ \tau \rightarrow \nu_\tau \begin{array}{l} \text{even} \\ \text{odd} \end{array} \right]}{ds} = \frac{G_\mu^2 V_{ud}^2}{8\pi m_\tau^3} (m_\tau^2 - s)^2 \left[ (m_\tau^2 + 2s) \begin{array}{l} \rho_V(s) \\ \rho_A(s) \end{array} + m_\tau^2 \begin{array}{l} 0 \\ \rho_A^{(0)} \end{array} \right], \quad (11)$$

and the corresponding  $n\pi$  branching ratio is

$$B_{n\pi} = \frac{G_\mu^2 V_{ud}^2 m_\tau^2}{8\pi \Gamma_{\tau \rightarrow \text{all}}} I_{n\pi} \quad \text{with} \quad I_{n\pi} = \int_{(nm_\pi)^2}^{m_\tau^2} ds \left[ 1 - \frac{s}{m_\tau^2} \right]^2 \left[ 1 + \frac{2s}{m_\tau^2} \right] \rho_{n\pi}(s). \quad (12)$$

In addition to the Particle Data Group (hereafter PDG) [10], the primary sources for  $\tau$  decay data are the ARGUS [11] and CLEO [12] detectors, via the reaction  $e^+e^- \rightarrow \tau^+\tau^-$ , and the CERN Large Electron-Positron Collider (LEP) detectors [13] via the decay  $Z^0 \rightarrow \tau^+\tau^-$ . A review of  $\tau$  physics up to 1988 is given by Barish and Stroynowski [14]. Experimental aspects of  $\tau$  decay continue to be presented up to the most recent conferences [15–17].

The next two relations  $W1$  and  $W2$  are, respectively, the first and second Weinberg sum rules [5,6]. The final sum rule  $W3$  is a formula for the  $\pi^\pm$ - $\pi^0$  mass splitting in the chiral limit [7]. Although apparently containing an arbitrary energy scale  $\Lambda$ , this sum rule is actually independent of  $\Lambda$  by virtue of  $W2$ . For reference, we have displayed the *physical* value of the nonzero entries which appear on the right-hand side of the chiral sum rules. These quantities have slightly shifted values in a chiral invariant world. This point is discussed at the end of Sec. III.

We note in passing that the current correlators defined in Eqs. (3) and (4) have been the subject of much recent attention. Several analyses have been carried out of hadron production in  $\tau$ -lepton decay in order to obtain a determination of  $\alpha_s(m_\tau)$ , the running strong fine-structure constant evaluated at the  $\tau$  mass scale [8].

### III. DATA INPUTS

It is possible, in principle, to analyze the chiral sum rules on the basis of pure theory. For example, in the original derivation of  $W3$ , the pion electromagnetic mass difference was estimated by using  $\rho(770)$  and  $a_1(1100)$  contributions to saturate the vector and axial-vector spectral functions [7]. However, a more sound procedure is to use data from  $\tau$  lepton semileptonic decays into pions and/or pion production in  $e^+e^-$  annihilations.

The rate for  $\tau$  decay into an even or odd number of pions at invariant squared energy  $s$  is given by [9]

At first, using  $e^+e^-$  annihilation data to test the chiral sum rules would appear to be problematic. Although the range of energy is (at least, in principle) unlimited, the production mechanism involves the electromagnetic current and so is generally a mixture of the needed isospin-1 component and an unwanted isospin-0 component. However, for final states which consist of an even number of pions it is only the isovector electromagnetic current which contributes. This is a consequence of

the  $G$ -parity relation  $G_{n\pi} = (-)^n$ , together with the property that any  $n\pi$  final state produced by the action of the electromagnetic current on the vacuum must have charge conjugation  $C = -1$ . Since  $G = C(-)^I$ , it follows that  $I = 1$  for  $n$  even. Of course, the isospin components which are measured in  $e^+e^-$  scattering and  $\tau$  decay are distinct, having  $I_3 = 0$  and  $1 - i2$ , respectively. The corresponding  $2\pi$  and  $4\pi$  states are related by

$$\begin{aligned} T_- |\pi^+ \pi^- \rangle &= \sqrt{2} |\pi^0 \pi^- \rangle, \\ T_- |2\pi^+ 2\pi^- \rangle &= 2\sqrt{2} |\pi^0 \pi^+ 2\pi^- \rangle, \\ T_- |\pi^+ \pi^- 2\pi^0 \rangle &= \sqrt{2} |\pi^- 3\pi^0 \rangle + 2\sqrt{2} |\pi^+ \pi^0 2\pi^- \rangle. \end{aligned} \quad (13)$$

Extraction of the  $n\pi$  component of  $\rho_V(s)$  from  $e^+e^-$  data proceeds via the relation

$$\rho_V^{n\pi}(s) = \frac{1}{16\pi^3 \alpha^2} s \sigma_{I=1}^{n\pi}(s). \quad (14)$$

For the specific case of two-pion production, the  $e^+e^-$  annihilation data is often expressed in terms of the pion electromagnetic form factor  $F^{\pi\pi}(s)$  evaluated at squared energy  $s$ . In this notation, one has

$$\rho_V^{2\pi}(s) = \frac{1}{48\pi^2} \left[ 1 - \frac{4m_\pi^2}{s} \right]^{3/2} |F^{\pi\pi}(s)|^2. \quad (15)$$

A plot of the pion form factor in the timelike region appears in Fig. 1. Early results on pion production in  $e^+e^-$  scattering is summarized in Ref. [18]. Experiments at Frascati, Orsay, and Novosibirsk have continued to supply data [19–26].

As a whole,  $\tau$  and  $e^+e^-$  data reveal that each of the multipion contributions rises fairly sharply from threshold to a peak value and then falls rather more slowly. At energies below 2 GeV, the role of meson resonances is significant. Thus, the  $2\pi$  contribution has the familiar narrow resonant structure of  $\rho(770)$ , the  $3\pi$  modes are dominated by  $a_1(1260)$ , and the  $4\pi$  sector is influenced by  $\rho(1450)$  and  $\rho(1700)$ . Although lacking a detailed dynamical understanding of higher multiplicity distributions, we can anticipate their form as a consequence of general physical considerations. They will occur sequen-

tially in mass (due to increasingly higher mass thresholds), exhibit slowly decreasing peak values (from competition with other channels as constrained by unitarity), and become increasingly broad (since phase space grows with particle number). As energy increases, one soon enters the asymptotic domain and the sum over all modes becomes featureless, in a manner similar to the total  $e^+e^-$  hadronic cross section.

Let us now present a critique of the current status for various individual contributions:

#### A. $\tau$ lepton properties

The most recent compilation given by PDG for the primary  $\tau$  lepton properties of mass ( $m_\tau$ ), lifetime ( $\tau_\tau$ ), and electron branching ratio  $B_e \equiv \Gamma_{\tau \rightarrow e \nu_\tau \bar{\nu}_e} / \Gamma_{\tau \rightarrow \text{all}}$  are

$$m_\tau^{\text{PDG}} \simeq 1.784 \text{ GeV}, \quad \tau_\tau^{\text{PDG}} \simeq 305 \text{ fs}, \quad B_e^{\text{PDG}} \simeq 0.1793. \quad (16)$$

However, there have been recent downward revisions to [27]

$$m_\tau \simeq 1.777 \text{ GeV}, \quad \tau_\tau \simeq 297 \text{ fs}, \quad B_e \simeq 0.1771, \quad (17)$$

and these are the values that we shall use throughout our analysis. Observe that there is a slight inconsistency between the listed central values for  $m_\tau$ ,  $\tau_\tau$ , and  $B_e$  in Eq. (12). As a result, the theoretical constraint

$$B_e = 0.06125 \frac{\tau_\tau}{10^{-13} \text{ sec}} \quad (18)$$

is not exactly satisfied. Thus, the relation between  $n\pi$  branching ratios and spectral functions in Eq. (12) depends on which of the following relations is assumed,

$$(i) B_{n\pi} = 4.39 \frac{\tau_\tau}{10^{-13} \text{ sec}} I_{n\pi}$$

or (19)

$$(ii) B_{n\pi} = 71.31 B_e I_{n\pi}.$$

Throughout this paper, we shall for definiteness assume that  $B_e = 0.1771$  in our numerical work. This value is an average of the value in Eq. (16) and the recent experimental determination cited in Ref. [28].

#### B. Two-pion component

Data for  $\rho_V^{2\pi}$  comes from the  $\pi^- \pi^0$  part of the one-prong  $\tau$  decay [11,29], and from the  $\pi^+ \pi^-$  final state in  $e^+e^-$  scattering [19,21,26,33]. The consistency of  $\tau$  decay and  $e^+e^-$  annihilation results in the vicinity of the  $\rho(776)$  peak has been verified by Gan in Ref. [30]. We display in Fig. 2 the two-pion spectral function  $\rho_V^{2\pi}(s)$  as inferred from the pion form factor data of Fig. 1. Numerical integration of  $\rho_V^{2\pi}$  yields a  $2\pi$  branching ratio of  $B_{2\pi} = 0.247$ . There are also recent determinations of the  $h^- \pi^0$  (where  $h$  is a hadron) and  $\pi^- \pi^0$  branching ratios by CLEO [12] and LEP [13],

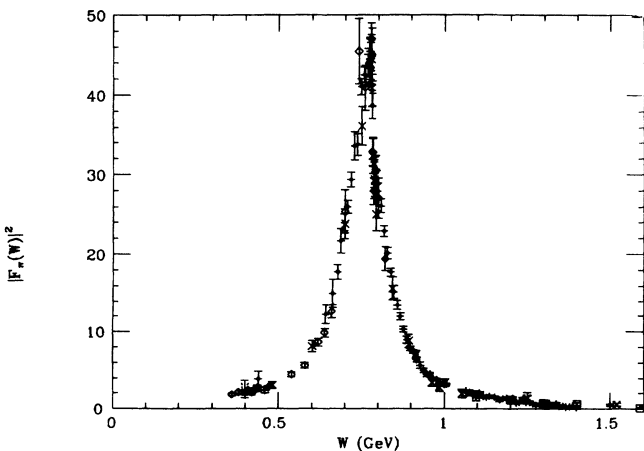
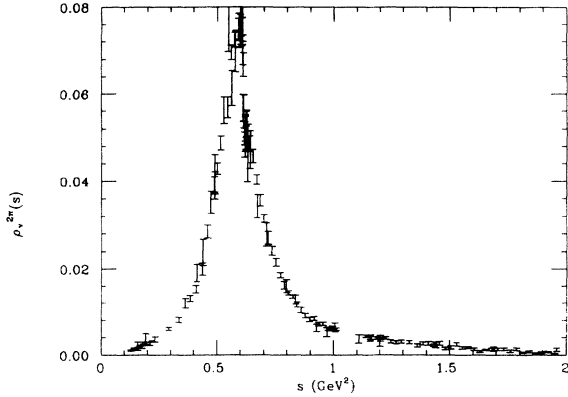


FIG. 1. Timelike pion form factor.

FIG. 2.  $2\pi$  vector spectral function.

$$\begin{aligned}
 B_{h^-\pi^0}^{\text{CLEO}} &= 0.2483 \pm 0.0015 \pm 0.0053, \\
 B_{h^-\pi^0}^{\text{LEP}} &= 0.243 \pm 0.008, \\
 B_{\pi^-\pi^0}^{\text{CLEO}} &= 0.2435 \pm 0.0055,
 \end{aligned} \tag{20}$$

where the  $\pi^-\pi^0$  value is inferred by subtracting off the  $K^{*-}$  branching ratio from that of  $h^-\pi^0$ . The above are in reasonable accord with the value cited by the PDG [10], which is based on earlier data.

All in all, the two-pion part of the vector current spectral function is well determined. As we shall now see, although much is known about the three- and four-pion distributions, more experimental input would be welcome.

### C. Three-pion component

We denote branching ratios for the two  $3\pi$  modes in  $\tau$  decay as  $B_{\pi^+2\pi^-}$  and  $B_{\pi^-2\pi^0}$ . Basic isospin considerations imply the inequalities [31]

$$\frac{1}{2} \leq \frac{B_{\pi^+2\pi^-}}{B_{3\pi}} \leq \frac{4}{5} \quad \text{and} \quad \frac{1}{5} \leq \frac{B_{\pi^-2\pi^0}}{B_{3\pi}} \leq \frac{1}{2}. \tag{21}$$

PDG lists the three-hadron branching ratios based on a number of experiments as

$$B_{h^+2h^-} = 0.084 \pm 0.004 \tag{22}$$

and

$$B_{h^-\pi^0} = 0.103 \pm 0.009.$$

CLEO [12] and LEP [13] have recently announced the results

$$\begin{aligned}
 B_{h^-\pi^0}^{\text{CLEO}} &= 0.0821 \pm 0.0015 \pm 0.0038 \pm 0.0028, \\
 B_{h^-\pi^0}^{\text{LEP}} &= 0.104 \pm 0.008, \\
 B_{h^+2h^-}^{\text{LEP}} &= 0.0949 \pm 0.0036 \pm 0.0063.
 \end{aligned} \tag{23}$$

Collectively, these imply that  $B_{\pi^+2\pi^-} \simeq B_{\pi^-2\pi^0}$  and indicate a total  $3\pi$  branching ratio of 16–19%. For definiteness, we shall assume that both modes have equal

decay rates and employ total three-pion branching ratios in this same range. This is in accord with the findings of Davier who, in a review of early and recent  $3\pi$  branching ratio determinations, summarizes the current situation as [17]

$$B_{\pi^+2\pi^-} = B_{\pi^-2\pi^0} = 0.0903 \pm 0.0036, \tag{24}$$

but at the same time makes the cautionary remark the “extreme care should be exercised when using world average values for branching ratios.”

The equality of  $\Gamma_{\pi^+2\pi^-}$  and  $\Gamma_{\pi^-2\pi^0}$  is expected of a final state which is dominated by the  $A_1$  resonance. The isospin decomposition

$$|A_1\rangle = \frac{1}{\sqrt{2}} |\rho^0\pi^-\rangle - \frac{1}{\sqrt{2}} |\rho^-\pi^0\rangle \tag{25}$$

shows that the  $\pi^+2\pi^-$  (from the first term) and the  $\pi^-2\pi^0$  (from the second term) final states will occur with equal probability.

As regards the spectral function  $\rho_A^{3\pi}$ , reconstruction from experiment would require  $3\pi$  mass distributions for both  $\pi^+2\pi^-$  and  $\pi^-2\pi^0$  modes. None of the latter exists. However, in view of  $A_1$  dominance it suffices to know just the  $\pi^+2\pi^-$  spectrum. We refer the reader to Ref. [14] for histograms of the  $3\pi$  mass distribution measured some time ago by the DELCO, MAC, and MARK II detectors. The literature also contains an early ARGUS determination [11], corresponding to the rather small branching ratio  $B_{\pi^+2\pi^-} = 0.056 \pm 0.007$ . In this paper, we shall employ recent ARGUS data [32] to determine  $\rho_A^{3\pi}$ . From the number of counts  $\Delta N$  per energy bin  $\Delta E$ , one can construct the  $3\pi$  spectral function via

$$\begin{aligned}
 \rho_A^{3\pi}(s) &= \frac{m_\tau^2}{24\pi^2 V_{ud}^2} \frac{B_{3\pi}}{B_e} \frac{1}{(1-s/m_\tau^2)^2 (1+2s/m_\tau^2)} \\
 &\times \frac{1}{2EN_{\text{tot}}} \frac{\Delta N}{\Delta E}, \tag{26}
 \end{aligned}$$

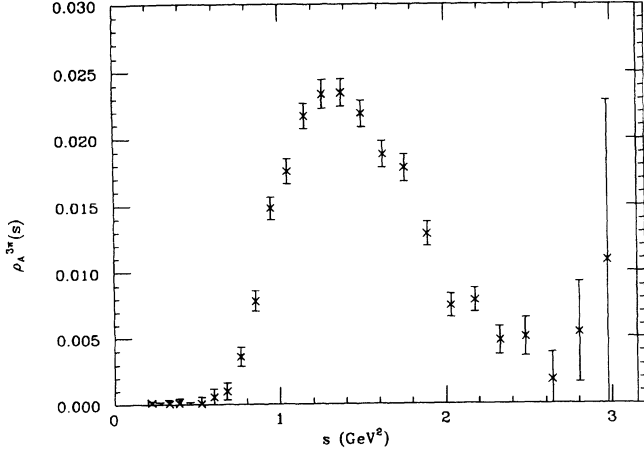
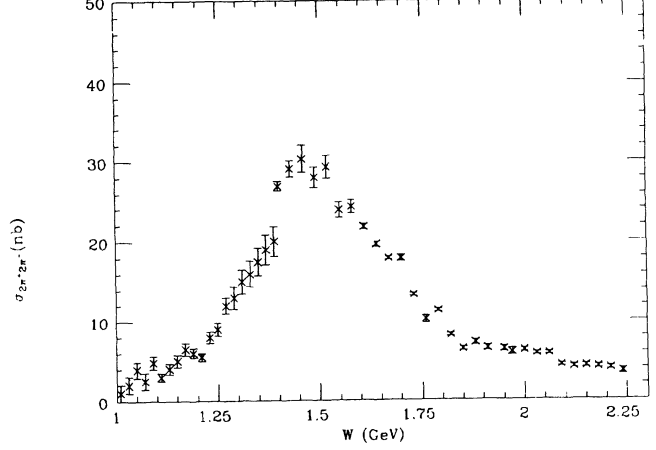
where  $E = \sqrt{s}$ . Upon taking  $B_{3\pi} = 0.17$  rather than the value given in Ref. [32] (which would imply  $B_{3\pi} = 0.13$ ), we obtain the spectral function shown in Fig. 3. The large error bars near the endpoint occur because one must divide the number of counts per energy bin by a phase space factor which vanishes at  $s = m_\tau^2$ . Even so, it is clear from Fig. 3 that  $\tau$  decay data is able to cover essentially all the region where  $\rho_A^{3\pi}$  is nonvanishing.

### D. Four-pion component

In  $\tau$  decay, there are two  $4\pi$  modes,  $\pi^-3\pi^0$  and  $\pi^+\pi^02\pi^-$ . The corresponding four-pion final states in  $e^+e^-$  scattering are  $2\pi^+2\pi^-$  and  $\pi^+\pi^-2\pi^0$ . The four-pion spectral function measured in  $\tau$  decay can be decomposed as

$$\rho_V^{4\pi}(s) = \rho_V^{+--0}(s) + \rho_V^{-000}(s), \tag{27}$$

where the quantities on the right-hand side are inferred from the four-pion mass distributions in the  $\pi^-3\pi^0$  and  $\pi^+\pi^02\pi^-$  modes. It is also possible to obtain the quantities  $\rho_V^{+--0}$  and  $\rho_V^{-000}$  from  $e^+e^- \rightarrow 4\pi$  cross sections via

FIG. 3.  $3\pi$  axial-vector spectral function.FIG. 4. Cross section for  $e^+e^- \rightarrow 2\pi^+2\pi^-$ .

the relations

$$\rho_V^{-000}(s) = \frac{1}{32\pi^3\alpha^2} s \sigma_{2\pi^+2\pi^-}, \quad (28)$$

$$\rho_V^{+-0}(s) = \frac{1}{32\pi^3\alpha^2} s (\sigma_{2\pi^+2\pi^-} + 2\sigma_{\pi^+\pi^-2\pi^0}). \quad (29)$$

The set of  $\pi^-3\pi^0$  and  $h^- \geq 3\pi^0$   $\tau$  decay branching ratios taken from recent conference presentations Refs. [12,13] and the average cited by the PDG [10] provide a reasonably consistent picture,

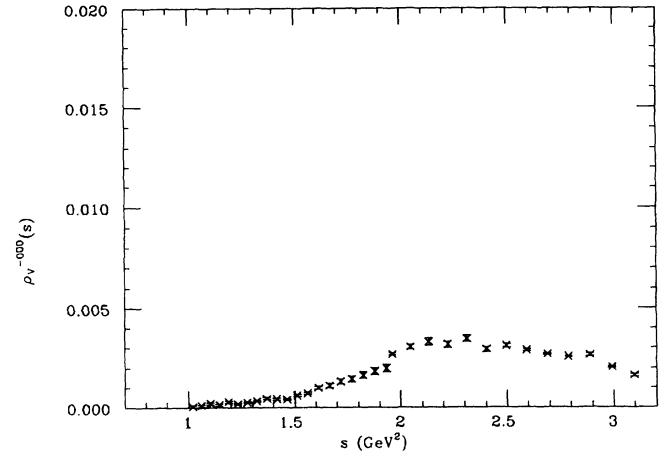
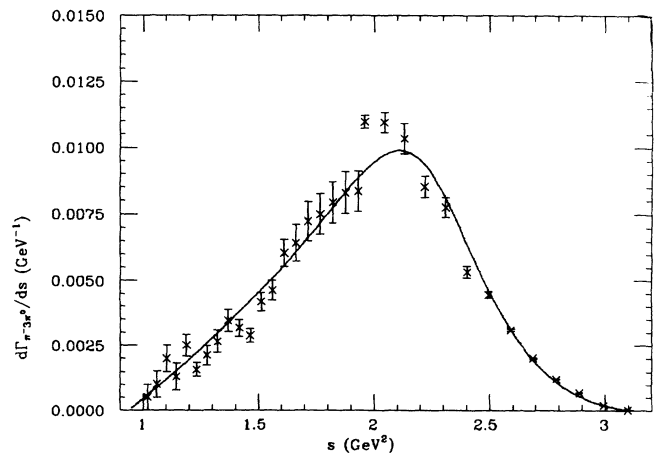
$$\begin{aligned} B_{h^-3\pi^0}^{\text{CLEO}} &= 0.0098 \pm 0.0007 \pm 0.0012 \pm 0.0003, \\ B_{h^- \geq 3\pi^0}^{\text{LEP}} &= 0.0153 \pm 0.004 \pm 0.006, \\ B_{h^- \geq 3\pi^0}^{\text{PDG}} &= 0.027 \pm 0.009, \end{aligned} \quad (30)$$

implying  $B_{\pi^-3\pi^0} \simeq 0.01$ . To our knowledge, there is no published *spectral* information from  $\tau$  decay data for the  $\tau \rightarrow \pi^-3\pi^0\nu_\tau$  mode. However, we can obtain  $\rho_V^{-000}(s)$  from  $\sigma_{2\pi^+2\pi^-}$  as in Eq. (28). The set of  $2\pi^+2\pi^-$  cross-section data taken from Ref. [22] (for  $\sqrt{s} < 1.4$  GeV) and from Refs. [20,21] (for  $\sqrt{s} > 1.4$  GeV) is displayed in Fig. 4. Note that Fig. 4 clearly demonstrates how  $\rho_V^{4\pi}$  must extend beyond  $s = m_\tau^2$ , i.e.,  $\tau$  decay alone cannot determine the  $4\pi$  spectral function over its full range. The resulting  $\rho_V^{-000}$  obtained in this manner is shown in Fig. 5. From this, we predict the  $\pi^-3\pi^0$  *mass spectrum* to have the form shown in Fig. 6, where a smooth curve has been added to help guide the eye. Integrating this mass spectrum leads to a branching ratio  $B_{\pi^-3\pi^0} \simeq 0.009$ , in good agreement with the values of Eq. (30).

Turning to the larger  $\pi^+2\pi^-\pi^0$   $\tau$  decay mode, we cite the branching ratio values appearing in Refs. [13,10,16],

$$\begin{aligned} B_{h^+2h^- \geq 1\pi^0}^{\text{LEP}} &= 0.0489 \pm 0.008, \\ B_{\pi^+2\pi^-\pi^0}^{\text{ARGUS}} &= 0.054 \pm 0.004 \pm 0.005, \\ B_{h^+2h^- \geq 1\pi^0}^{\text{PDG}} &= 0.053 \pm 0.004, \end{aligned} \quad (31)$$

where the ARGUS value is preliminary. Two of these values include unknown amounts of strange particle con-

FIG. 5.  $\rho_V^{-000}$  inferred from  $e^+e^-$  scattering.FIG. 6. Predicted  $4\pi$  mass spectrum in  $\tau \rightarrow \pi^-3\pi^0\nu_\tau$ .

tributions. Allowing for such non- $4\pi$  contributions, the PDG and LEP values indicate a  $\pi^+2\pi^-\pi^0$  branching ratio in the 0.040–0.050 range. We are aware of just one published  $\pi^+2\pi^-\pi^0$  mass spectrum measurement, an ARGUS analysis (Ref. [33]), which cites the branching ratio  $B_{\pi^+2\pi^-\pi^0} = 0.042 \pm 0.005 \pm 0.009$ . This value is smaller than, although not inconsistent with, the more recent ARGUS value of Eq. (31). Using an appropriate binning procedure, we can construct the full  $4\pi$  spectral function  $\rho_V^{4\pi}(s)$  over the restricted energy region  $s < m_\tau^2$  by combining the  $\pi^+2\pi^-\pi^0$   $\tau$  data together with the  $2\pi^+2\pi^-$  cross sections. The result is shown in Fig. 7, together with an asymmetric Breit-Wigner fitting curve (see Sec. IV).

Alternatively, one could use the combination of cross sections as in Eq. (29) to determine the total  $4\pi$  spectral function. In principle, at least, this procedure can provide the  $4\pi$  spectral function over a larger energy interval.  $\pi^+\pi^-2\pi^0$  cross-section data taken from Ref. [25] (for  $\sqrt{s} < 1.4$  GeV) and from Ref. [20] (for  $\sqrt{s} > 1.4$  GeV) are displayed in Fig. 8. These turn out to imply a  $\pi^+2\pi^-\pi^0$   $\tau$  decay branching ratio somewhat smaller than the recent determinations cited in Eq. (31). For this reason, we have chosen to base our analytical work on the determination of  $\rho_V^{4\pi}(s)$  as shown in Fig. 7.

### E. Higher components

The five-pion component in  $\tau$  decay involves the branching ratios  $B_{\pi^-4\pi^0}$ ,  $B_{3\pi^-2\pi^+}$ , and  $B_{2\pi^-\pi^+2\pi^0}$ . Isospin constraints for these modes are

$$0 \leq \frac{B_{\pi^-4\pi^0}}{B_{5\pi}} \leq \frac{3}{10}, \quad 0 \leq \frac{B_{3\pi^-2\pi^+}}{B_{5\pi}} \leq \frac{8}{35}, \quad (32)$$

$$\frac{8}{35} \leq \frac{B_{2\pi^-\pi^+2\pi^0}}{B_{5\pi}} \leq 1.$$

At present, Refs. [12,10,16] provide the following branching ratio determinations,

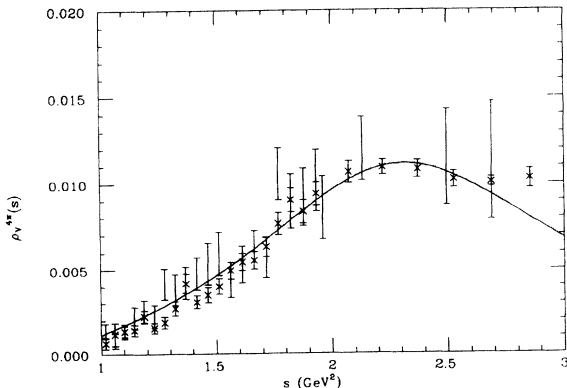


FIG. 7.  $\rho_V^{4\pi}$  from  $\tau$  decay and  $e^+e^-$  scattering.

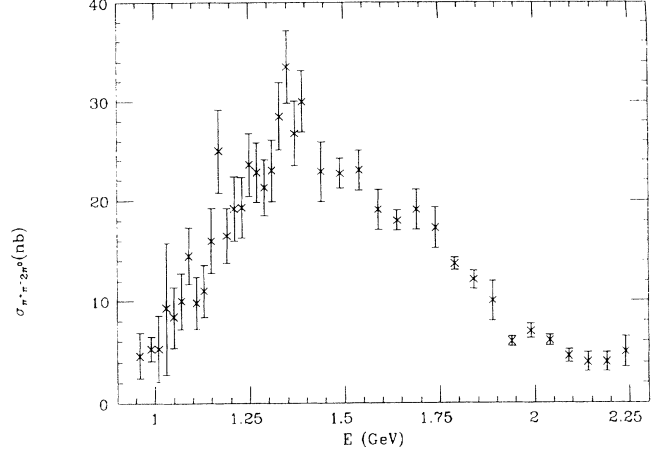


FIG. 8. Cross section for  $e^+e^- \rightarrow \pi^+\pi^-2\pi^0$ .

$$B_{h^-4\pi^0}^{\text{CLEO}} = 0.0015 \pm 0.0004 \pm 0.0005 \pm 0.0001,$$

$$B_{3h^-2h^+}^{\text{PDG}} = 0.00056 \pm 0.00016, \quad (33)$$

$$B_{2\pi^-\pi^+2\pi^0}^{\text{ARGUS}} = 0.0054 \pm 0.0005 \pm 0.0008.$$

Noting that  $B_{3\pi^-2\pi^+} \leq B_{3h^-2h^+}$ , we find that these values are consistent with the bounds of Eq. (32). However, the isospin bounds do not imply any useful information for disentangling  $B_{3\pi^-2\pi^+}$  from  $B_{3h^-2h^+}$ . To our knowledge, the above branching ratios are the only  $5\pi$  data currently available. To obtain useful spectral information for the  $5\pi$  mode requires a substantial number of events, e.g., as would be generated from a  $\tau$  factory.

Some  $6\pi$  spectral information is available from  $e^+e^-$  scattering and some  $6\pi$  branching ratio information is available, but in view of the paucity of  $5\pi$  data we have not included this sector in the analysis described in this paper.

Although our statement of the chiral sum rules in Sec. II refers to the limit of massless quarks, the data reviewed in this section are taken in the real world of  $m_{u,d} \neq 0$ . In principle, we might attempt to perform corrections on the data set with an eye towards working in the chiral limit. For example, it is apparent that taking  $m_\pi \rightarrow 0$  would induce minor shifts in resonance masses and phase space. However, we anticipate that such effects would be of order  $m_\pi^2/\Lambda^2$  with  $\Lambda \simeq 1$  GeV. Since such changes are much smaller than the present uncertainty in the data, it seems most prudent not to try to model the effect of finite  $m_{u,d}$  effects. Thus, we shall use the unmodified experimental information in our phenomenological analysis.

## IV. THEORETICAL CONSTRAINTS

Although the vector and axial-vector spectral functions are not theoretically prescribed for all values of  $s$ , it is possible to place constraints on their low- and high-energy limits.

We begin by taking the Fourier transform of Eq. (3),

$$\begin{aligned}\delta_{ab}\Pi_{\mu\nu}^V(q^2) &= i \int d^4x \exp(iq \cdot x) \langle 0 | T [V_a^\mu(x) V_b^\nu(0)] | 0 \rangle \\ &\equiv \delta_{ab}(q_\mu q_\nu - g_{\mu\nu} q^2) \Pi_V(q^2),\end{aligned}\quad (34)$$

and of Eq. (4),

$$\begin{aligned}\delta_{ab}\Pi_{\mu\nu}^A(q^2) &= i \int d^4x \exp(iq \cdot x) \langle 0 | T [A_a^\mu(x) A_b^\nu(0)] | 0 \rangle \\ &\equiv \delta_{ab}(q_\mu q_\nu - g_{\mu\nu} q^2) \Pi_A(q^2) \\ &\quad - q^\mu q^\nu \Pi_A^{(0)}(q^2).\end{aligned}\quad (35)$$

In the chiral limit, the spin-0 axial contribution  $\Pi_A^{(0)}(q^2)$  is given entirely by the pion pole. The correlators  $\Pi_{V,A}(q^2)$  are the real parts of analytic functions whose imaginary parts are the spectral functions  $\rho_{V,A}(s)$ . Of interest to us are the dispersion relations involving the difference of vector and axial-vector quantities,

$$\Pi_V(q^2) - \Pi_A(q^2) = \frac{32\pi}{9} \frac{\langle \sqrt{\alpha_s \bar{q}q} \rangle_0^2}{q^6} \left[ 1 + \frac{\alpha_s(q^2)}{4\pi} \left[ \frac{247}{12} + \ln \left[ \frac{\mu^2}{-q^2} \right] \right] \right]. \quad (38)$$

It turns out that theory also predicts the low-energy or threshold behavior of the vector and axial-vector correlators. However, in this case it is the machinery of chiral perturbation theory that is invoked to show [36]

$$\begin{aligned}\Pi_V(q^2) - \Pi_A(q^2) &= \frac{F_\pi^2}{q^2} + \frac{1}{48\pi^2} \left[ \ln \left[ \frac{\mu^2}{-q^2} \right] + \frac{5}{3} \right] \\ &\quad - L_{10}^{(r)}(\mu),\end{aligned}\quad (39)$$

where  $L_{10}^{(r)}(\mu)$  is defined in Eq. (10).

The above statements all involve the correlators  $\Pi_{V,A}$ . Similar threshold and asymptotic constraints can be placed on the spectral functions  $\rho_{V,A}(s)$ . Thus, as stated in Ref. [36] the threshold behavior ( $s \rightarrow 4m_\pi^2$ ) of  $\rho_V(s)$  and  $\rho_A(s)$  is

$$\rho_V(s) \sim \frac{1}{48\pi^2} \left[ 1 - \frac{4m_\pi^2}{s} \right]^{3/2} \theta(s - 4m_\pi^2) + O(p^2), \quad (40)$$

$$\rho_A(s) \sim O(p^2). \quad (41)$$

Later in this section, we shall sharpen the threshold result for  $\rho_A$  by specifying the  $3\pi$  threshold contribution in more detail. The perturbative result for the asymptotic limit  $s \rightarrow \infty$  of the individual  $\rho_{V,A}$  to leading order is

$$\rho_{V,A}(s) \sim \frac{1}{8\pi^2} \left[ 1 + \frac{\alpha_s(s)}{\pi} \right]. \quad (42)$$

Finally, Eq. (38) determines the asymptotic form of  $\rho_V(s) - \rho_A(s)$  to be

$$\rho_V(s) - \rho_A(s) \sim \frac{C}{s^3} \approx \frac{8}{9} \frac{\alpha_s \langle \sqrt{\alpha_s \bar{q}q} \rangle_0^2}{s^3} \quad \text{for large } s. \quad (43)$$

$$\begin{aligned}\Pi_V(q^2) - \Pi_A(q^2) &= \frac{F_\pi^2}{q^2} + \int_0^\infty ds \frac{\rho_V(s) - \rho_A(s)}{s - q^2 - i\epsilon} \\ &= \frac{1}{q^2} \int_0^\infty ds s \frac{\rho_V(s) - \rho_A(s)}{s - q^2 - i\epsilon}.\end{aligned}\quad (36)$$

In our normalization, the behavior of the individual  $\Pi_{V,A}(q^2)$  to leading order at large  $q^2$  is

$$\Pi_{V,A}(q^2) \sim \frac{1}{8\pi^2} \left[ 1 + \frac{\alpha_s(q^2)}{\pi} \right] \ln \left[ \frac{\mu^2}{-q^2} \right], \quad (37)$$

where  $\mu$  is the renormalization scale. In order to determine the difference  $\Pi_V(q^2) - \Pi_A(q^2)$  for  $q^2$  large but finite, one must go beyond the form in Eq. (37). From the operator product expansion of vector and axial-vector currents, we learn that the asymptotic dependence is  $O(q^{-6})$  and the local operators which control this behavior are the four-quark condensates [34,35]. In the approximation of vacuum saturation, one finds

Note that the difference of the spectral functions is of order  $\alpha_s^2$ . Our analysis of the chiral sum rules will require a numerical value for the coefficient  $C$  of the  $s^{-3}$  term. From the estimate

$$\langle \sqrt{\alpha_s \bar{q}q} \rangle_0^2 \simeq (0.24 \text{ GeV})^6 \simeq 1.9 \times 10^{-4} \text{ GeV}^6 \quad (44)$$

and taking  $\alpha_s \simeq 0.2$ , we obtain

$$C \simeq 3.4 \times 10^{-5} \text{ GeV}^6. \quad (45)$$

The magnitude of this quantity is obviously model dependent and quite possibly will be modified by future work. However, even folding in uncertainties of the vacuum condensates, it is clear that the coefficient of the  $s^{-3}$  term is very small, and that  $\rho_V - \rho_A$  approaches zero very quickly at large  $s$ . Even if one imagines  $\rho_V(s) - \rho_A(s)$  to exhibit increasingly damped oscillations indefinitely, duality suggests that Eq. (43) captures the correct average behavior. As we shall see, the asymptotic constraint of Eq. (43) will have significant impact in the analysis of the chiral sum rules to come.

The results presented in this section are well known, and collectively they represent a fairly powerful set of conditions regarding how the chiral correlators can behave. Actually, additional thought can reveal even more. For example, let us employ the asymptotic behavior of Eq. (38) in the dispersion relation of Eq. (36). Expansion of the dispersion integral in powers of  $q^{-2}$  yields the sum rule

$$\frac{32\pi}{9} \langle \sqrt{\alpha_s \bar{q}q} \rangle_0^2 = - \int_0^\infty ds s^2 [\rho_V(s) - \rho_A(s)]. \quad (46)$$

Some care must be taken to interpret this result correctly. Observe that Eq. (46) is valid to  $O(\alpha_s)$ . Since the  $O(s^{-3})$  tail of  $\rho_V(s) - \rho_A(s)$  is itself of higher order in  $\alpha_s$ , one

must subtract it off in this relation. Accordingly, we write

$$\frac{32\pi}{9} \langle \sqrt{\alpha_s \bar{q}q} \rangle_0^2 = - \int_0^\infty ds s^2 [\rho_V(s) - \rho_A(s)]', \quad (47)$$

where  $[\rho_V(s) - \rho_A(s)]'$  refers to the subtraction procedure just mentioned.

Finally, let us return now to the matter of the threshold behavior of  $\rho_A(s)$ . It is associated with the  $3\pi$  component. Using chiral Lagrangian methods [1], we have determined that in the chiral limit the threshold behavior is

$$\begin{aligned} \langle 0 | A^\mu(0) | \pi_{p_+}^+ \pi_{p_0}^0 \pi_{p_-}^- \rangle &= \frac{2}{3F_\pi} (p_+^\mu + p_-^\mu - 2p_0^\mu) \\ &\quad - \frac{3s_{+-} - s}{3F_\pi s} Q^\mu, \end{aligned} \quad (48)$$

where  $Q \equiv p_+ + p_- + p_0$ ,  $s \equiv Q^2$ , and  $s_{+-} \equiv (p_+ + p_-)^2$ . Upon rearrangement of terms, this can be expressed as

$$\langle 0 | A^\mu(0) | \pi_{p_+}^+ \pi_{p_0}^0 \pi_{p_-}^- \rangle = \frac{2}{F_\pi} \left[ \frac{Q p_0}{Q^2} Q^\mu - p_0^\mu \right]. \quad (49)$$

Observe that this obeys

$$\langle 0 | \partial_\mu A^\mu(0) | 3\pi \rangle = 0,$$

as must be the case since it is only the spin-1 part of the axial-vector current which contributes here. The threshold behavior of  $\rho_A^{3\pi}(s)$  can then be read off from the general form of Eq. (5) by first squaring Eq. (49) and integrating over  $3\pi$  phase space,

$$\rho_A^{3\pi}(s) = \frac{s}{96\pi(4\pi F_\pi)^2} + \dots \quad (50)$$

In practice, however, the very low  $s$  behavior for the  $3\pi$  state turns out to be less important in the chiral sum rules than the higher energy effect of the  $A1$  resonance.

## V. EMPIRICAL DETERMINATIONS OF CHIRAL SUM RULES

Before discussing our own methodology, we wish to take note of two interesting works involving aspects of chiral sum rules. In the earlier of these [37], spectral functions based on  $2\pi$ ,  $3\pi$ , and  $4\pi$  data extracted from  $\tau$  decay are used to study the sum rules  $W1$ ,  $W2$ , and  $W3$ . The associated spectral integrals are studied as a function of cutoff  $s_0$  for  $s_0 \leq 2.5 \text{ GeV}^2$ . However, the  $3\pi$  analysis was taken from Ref. [11] data, which as we have seen is not in agreement with a large number of more recent branching ratio measurements. In addition, the  $2\pi$  spectral function was too small in the vicinity of the  $\rho(770)$  peak by roughly a factor of 2. Interestingly, these two features combined to make the sum rules appear reasonably in agreement with expectations, although this result was fortuitous.

In the analysis of Ref. [38],  $2\pi$  and  $4\pi$  data are inferred from  $e^+e^-$  scattering, but the  $3\pi$  data again comes from Ref. [11]. In fitting these components, use is made of Breit-Wigner resonance forms with energy-dependent de-

cah widths. The particular form of energy dependence is taken from Lorentz-invariant phase space. The  $5\pi$  and higher components are parameterized to give rise to the asymptotic behavior

$$\rho_{V,A}(s) \sim \frac{5}{32\pi^2} \quad \text{and} \quad \rho_V - \rho_A \sim O(s^{-1}). \quad (51)$$

This disagrees with the chiral and operator product expansion results of Eqs. (42) and (43), respectively. The specific form in Ref. [38] used for the higher components is chosen to fit the sum rule  $W1$  exactly and the sum rule  $W0$  is evaluated in terms of the fit.

The summary given in Sec. III of available data demonstrates that there is hope for successfully extracting much about the spectral functions  $\rho_{V,A}(s)$  from experiment, but that our knowledge of them will always be limited. In view of the current database, we have decided that for the purpose of testing the chiral sum rules, it is most prudent to take the empirical  $2\pi$ ,  $3\pi$ , and  $4\pi$  modes explicitly into account, and to treat all higher components according to some reasonable prescription. We have followed two distinct approaches in doing so.

(i) *Numerical*: We ensure that the empirical databases for  $\rho_{V,A}(s)$  evolve smoothly in the variable  $s$  to the correct asymptotic limits by generating smooth curves separately for  $\rho_V$  and  $\rho_A$  which pass through the experimental data sets at low energy and which satisfy the asymptotic limits, while reproducing the four chiral sum rules.

(ii) *Analytical*: This actually encompasses a class of fits to the difference of spectral functions  $\rho_V - \rho_A$  in which all contributions higher than the four-pion sector are lumped into a single theoretical term. A convenient method for constructing the spectral functions this way is to start with a  $\delta$  function form, then introduce finite widths via Briet-Wigner representations, and finally modify these to a more realistic asymmetric form.

Let us consider each possibility in turn.

### A. Numerical representation

Surely the simplest method for generating acceptable global versions of  $\rho_{V,A}$  is to numerically smoothly join the low-energy empirical data with asymptotic theoretical information. A reasonable region for matching the two occurs at about  $s \simeq 4-5 \text{ GeV}^2$ . As we have already seen, the constraint of Eq. (42) reveals that the spectral functions approach a nonzero constant at infinite energy, with an additive correction factor proportional to  $\alpha_s(s)$ . In general, we expect the large  $s$  behavior

$$\rho_{V,A}(s) = \rho_0^{V,A} + \frac{\rho_1^{V,A}}{s} + \frac{\rho_2^{V,A}}{s^2} + \dots \quad (52)$$

We can obtain a determination of the dominant power correction in the large  $s$  limit as follows. Using an operator product expansion, Braaten, Narison, and Pich have displayed the structure of the correlators  $\Pi_{V,A}$  for Euclidean momenta  $-Q^2$  in Appendix A of their paper [8],



$$\Pi_{V,A}(-Q^2) = a_0^{V,A}(Q) + \frac{a_1^{V,A}(Q)}{Q^2} + \frac{a_2^{V,A}(Q)}{Q^4} + \dots, \quad (53)$$

where  $s = -Q^2$  and each of the  $a_n^{V,A}(Q)$  is expandable in powers of  $\alpha_s(Q)$ . We require the imaginary part of this expression, analytically continued to timelike momenta. Since the  $O(Q^{-2})$  contribution to  $\Pi_{V,A}$  turns out to be proportional to quark mass, the coefficient  $\rho_1^{V,A}(s)$  vanishes in the chiral limit. Thus, the first nonvanishing sub-leading contribution is the  $O(Q^{-4})$  component, from which we extract the result

$$\rho_2^{V,A}(s) \sim \frac{11}{192\pi^2} \alpha_s^2 \left\langle \frac{\alpha_s}{\pi} G^2 \right\rangle_0 \text{ for large } s. \quad (54)$$

Let us estimate the magnitude of this quantity at  $s = 5 \text{ GeV}^2$ . The strong fine-structure constant is determined in terms of an assumed value for the QCD scale parameter,

$$\Lambda_{\text{QCD}} = 150 \text{ MeV} \Rightarrow \alpha_s(5 \text{ GeV}^2) \simeq 0.26 \quad (55)$$

and the gluon condensate from phenomenological applications of QCD sum rules,

$$\left\langle \frac{\alpha_s}{\pi} G^2 \right\rangle_0 = (0.02 \pm 0.01) \text{ GeV}^4. \quad (56)$$

Altogether, these values imply that the  $O(s^{-2})$  component to  $\rho_{V,A}$  has a tiny coefficient,

$$\rho_2^{V,A} \simeq 0.9 \times 10^{-5} \text{ GeV}^4. \quad (57)$$

As a result, even at the modest energy  $s \simeq 5 \text{ GeV}^2$  the  $O(s^{-2})$  term has a negligible effect. Of course, this common addition to  $\rho_V$  and  $\rho_A$  will cancel when the difference is taken and hence will not contribute to the chiral sum rules. In addition, the difference of the spectral functions was chosen to be compatible with the asymptotic constraint given in the previous section. Again the magnitude of this contribution is so small that it is essentially irrelevant at modest energies. Thus while we have made an effort to generate spectral functions with the right high-energy behavior, the precise value of the high-energy terms is not important since their numerical size is quite small.

Let us summarize our procedure at this point. We have generated numerical representations for  $\rho_V$  and  $\rho_A$  which fit all available data on multipion production, and which are compatible with the theoretical behavior expected at high energy, and which when integrated yield the correct experimental values for the four chiral sum rules. Although highly constrained at low and high energies, the spectral functions have a modest uncertainty in the  $s = 2-4 \text{ GeV}^2$  range, and this was exploited in order to precisely duplicate the expected values of the sum rules  $W0, W1, W2, W3$ . Of course, both this numerical procedure and the analytic one to follow are subject to the choice of input values. Given the uncertainties in especially the  $3\pi$  and  $4\pi$  branching ratios, we have explored a variety of possibilities. Corresponding to the input set

$$B_{2\pi} = 0.240, \quad B_{3\pi} = 0.165, \quad B_{4\pi} = 0.048, \quad (58)$$

curves for  $\rho_V, \rho_A$ , and  $\rho_V - \rho_A$  are displayed, respectively, in Figs. 9-11.

## B. Analytical representations

### 1. $\delta$ function

In the  $\delta$  function description, the spectral functions are

$$\rho_V(s) - \rho_A(s) = \sum_{k=1}^4 (-)^{k+1} F_k^2 \delta(s - m_k^2). \quad (59)$$

This representation of the spectral functions, although crude, provides a nice pedagogical example with which to organize one's thoughts. We begin by noting that there are two parameters per contribution, a mass  $m$  and a coupling  $F$ . In this approach, the four sum rules reduce to

$$W0 = \sum_{k=1}^4 (-)^{k+1} \frac{F_k^2}{m_k^2}, \quad (60)$$

$$W1 = \sum_{k=1}^4 (-)^{k+1} F_k^2 = F_\pi^2, \quad (61)$$

$$W2 = \sum_{k=1}^4 (-)^{k+1} m_k^2 F_k^2 = 0, \quad (62)$$

$$W3 = \sum_{k=1}^4 (-)^{k+1} m_k^2 F_k^2 \ln m_k^2, \quad (63)$$

and the  $\tau$  decay branching ratios become

$$B_k = 71.62 B_e F_k^2 \left[ 1 - \frac{m_k^2}{m_\tau^2} \right]^2 \left[ 1 + \frac{2m_k^2}{m_\tau^2} \right] \quad (k=1,2,3). \quad (64)$$

We can specify the mass parameters  $m_{1,2,3}$  from the observed  $n\pi$  ( $n=2,3,4$ ) distributions and the coupling strengths  $F_{1,2,3}$  from the observed branching ratios [cf. Eq. (12)]. Even in the extreme narrow width approximation of the  $\delta$  function representation, this step turns out to be a surprisingly accurate one, e.g., finite width effects modify the branching ratio relations by only a few percent.

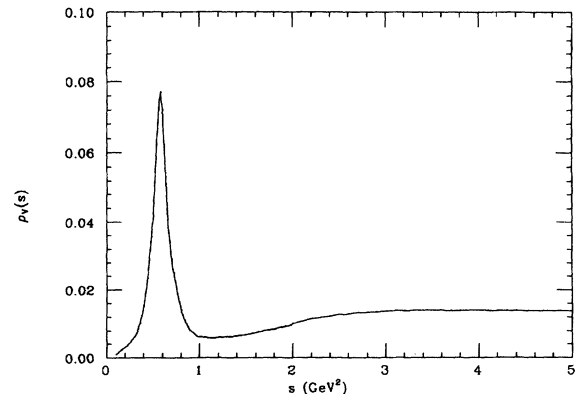
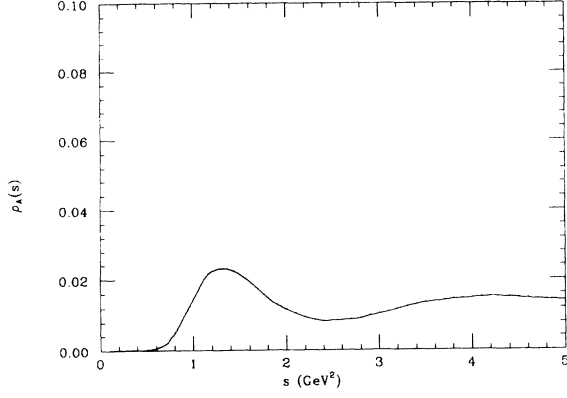


FIG. 9. Numerical fit to  $\rho_V$ .

FIG. 10. Numerical fit to  $\rho_A$ .

This leaves the problem of determining the coupling  $F_4$  and mass  $m_4$ . It seems reasonable to require that the sum rules  $W1$  and  $W2$  be obeyed exactly [cf. Eqs. (61) and (62)]. Thus we determine  $F_4$  from Eq. (61) and  $m_4$  from Eq. (62). Doing so leaves the remaining sum rules  $W0$  and  $W3$  as predictions.

## 2. Breit-Wigner

In the finite width Breit-Wigner (BW hereafter) extension of Eq. (59), the spectral functions are represented by

$$\rho_V(s) - \rho_A(s) = \sum_{k=1}^4 \frac{(-)^{k+1}}{\pi} \frac{F_k^2 m_k \Gamma_k}{(s - m_k^2)^2 + (m_k \Gamma_k)^2}. \quad (65)$$

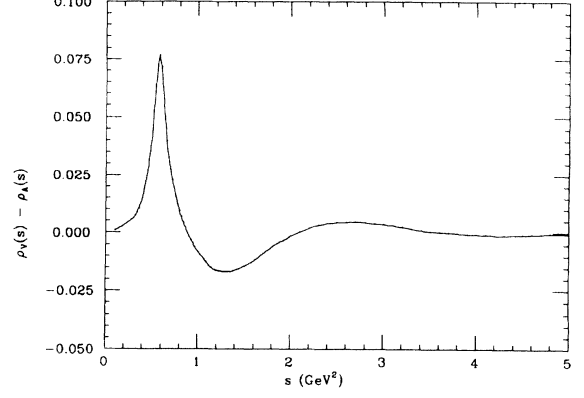
Each contribution still has mass and coupling parameters  $m_k$  and  $F_k$ , but now, in addition, a width  $\Gamma_k$ . In the most general Breit-Wigner resonance form, decay widths are taken to be energy dependent, e.g., the  $2\pi$  widths have the  $O(p^3)$  threshold behavior to reflect the  $P$ -wave nature of the  $2\pi$  system. However, in order to maintain a simplicity of description and the ability to represent each  $n\pi$  component in analytic form, we shall employ energy-

$$\begin{aligned} I_{\text{BW}}^{(1)} &\equiv \int_{s_0}^{\Lambda} ds s \rho_{\text{BW}}(s) \\ &= m^2 I_{\text{BW}}^{(0)} + F^2 r \left[ \ln \frac{\Lambda}{m} + 0.5 \ln \left( \frac{(1 - m^2/\Lambda)^2 + m^4 \pi^2 r^2 / \Lambda^2}{(1 - s_0/m^2)^2 + \pi^2 r^2} \right) \right]. \end{aligned} \quad (68)$$

By passing to the limit  $r=0$  of zero decay width, we regain the results of the  $\delta$ -function model.

Analogous to the procedure used in the  $\delta$ -function model, parameters for the first three BW poles are obtained by fitting to experimental data. In passing, we note that since a given spectral contribution has the asymptotic behavior  $O(s^{-2})$ , the *individual* BW spectral integrals for  $W2$  and  $W3$  are divergent. The numerator of the fourth pole is fixed by demanding that the  $O(s^{-2})$  asymptotic term in  $\rho_V - \rho_A$  vanish. This implies

$$\sum_{k=1}^4 (-)^{k+1} F_k^2 m_k \Gamma_k = 0. \quad (69)$$

FIG. 11. Numerical fit to  $\rho_V - \rho_A$ .

independent widths throughout.

An advantage of the  $\delta$ -function approach was the ability to express all the sum rules and the tau branching ratios in elementary form. This is still true in the BW approximation for the sum rules  $W0$ ,  $W1$ ,  $W2$ , and the  $\tau$  branching ratios. For example, working with a generic Breit-Wigner spectral function,

$$\rho_{\text{BW}}(s) = \frac{F^2 m^2 r}{(s - m^2)^2 + (m^2 \pi r)^2}, \quad (66)$$

where  $r \equiv \Gamma/(\pi m)$  is an expansion parameter for finite width effects, we can evaluate integrals such as

$$\begin{aligned} I_{\text{BW}}^{(0)} &\equiv \int_{s_0}^{\Lambda} ds \rho_{\text{BW}}(s) \\ &= F^2 \left[ 1 - \frac{1}{\pi} \arctan \frac{\pi r}{(\Lambda/m^2) - 1} \right. \\ &\quad \left. - \frac{1}{\pi} \arctan \frac{\pi r}{1 - (s_0/m^2)} \right] \end{aligned} \quad (67)$$

and

By virtue of this relation, the asymptotic behavior of the vector and axial-vector spectral functions becomes

$$\rho_V(s) - \rho_A(s) = \frac{C_{\text{BW}}}{s^3} + O(s^{-4}), \quad (70)$$

where

$$C_{\text{BW}} = \frac{2}{\pi} \sum_{k=1}^4 (-)^{k+1} F_k^2 m_k^3 \Gamma_k. \quad (71)$$

The constant  $C_{\text{BW}}$  may be considered either as a quantity to be fixed by Eq. (43) or as a prediction of the analysis.

We find it hard to see how any analytical study of the

sum rules could succeed without incorporating the above features or something similar. In our approach, all the chiral sum rules are convergent even though individual pole contributions may diverge. Moreover, the condition given by Eq. (69) ensures that our description has the smoothness in energy expected from duality.

### 3. Asymmetric Breit-Wigner

Although having the virtue of simplicity, the representation of Eq. (65) is deficient in several important respects. A Breit-Wigner form is symmetric about its resonant energy whereas the  $n\pi$  contributions to  $\rho_{V,A}$  exhibit asymmetric bumps. Besides, the BW contributions extend to energies lying below thresholds which characterize the various  $n\pi$  components.

An improved treatment can be realized in a variety of ways. One simple parameterization which treats the various components uniformly, yields a reasonable fit to data and allows us to maintain analytic control is

$$\rho_V(s) - \rho_A(s) = \sum_{k=1}^4 (-)^{k+1} \frac{P_k(s) F_k^2 m_k \Gamma_k}{(s - m_k^2)^2 + (m_k \Gamma_k)^2}. \quad (72)$$

The functions  $P_k(s)$  are polynomials

$$P_k(s) = \left[ 1 - \frac{s_k^2}{s^2} \right]^{n_k}, \quad (73)$$

each containing two parameters, a threshold energy  $s_k$  and an integer-valued exponent  $n_k = 1, 2, \dots$ . Although the choice  $n_k = 1$  is the simplest one, it yields an  $n\pi$  spectral function which rises linearly just above threshold. This does not appear to provide an adequate fit to the data, and thus we have used  $n_k = 2$  ( $k = 1, \dots, 4$ ). A fit of this type to the  $3\pi$  spectral function appears in Fig. 12.

Introduction of the polynomials  $P_k(s)$  will clearly lead to integrals involving inverse moments of Breit-Wigner forms,

$$I_{\text{BW}}^{(-n)} = \int_{s_0}^{\infty} ds \frac{\rho_{\text{BW}}(s)}{s^n}. \quad (74)$$

Although it is straightforward to evaluate such integrals

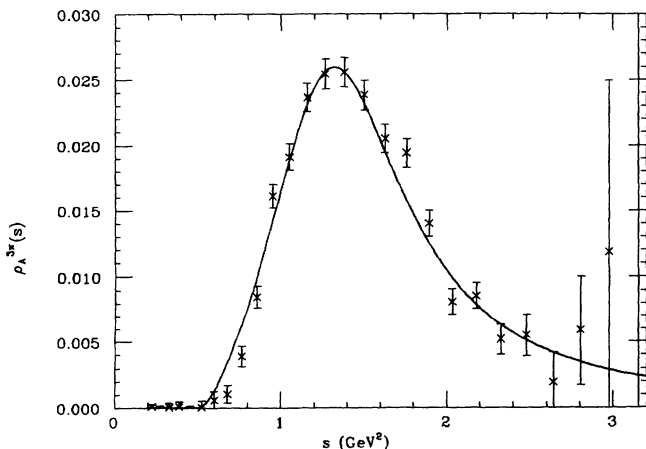


FIG. 12. Fit of asymmetric Breit-Wigner solution to  $3\pi$  spectral function.

analytically, the resulting expressions can be quite cumbersome. In practice, it is more efficient to employ the recursion relation

$$I_{\text{BW}}^{(-n)} = \frac{1}{m^4(1+\pi^2 r^2)} \left[ 2m^2 I_{\text{BW}}^{(-n+1)} - I_{\text{BW}}^{(-n+2)} + \frac{s_0^{-n+1}}{n-1} \right]. \quad (75)$$

Upon applying relations of this type, we have carried out the calculational program described earlier in this section. As stated earlier, because of the uncertainty in the experimental  $3\pi$  and  $4\pi$  contributions, we have performed the analysis for several different sets of  $\tau$  lepton branching ratios. Typical results are shown in Table I, where we display both input values (parameters for the  $2\pi$ ,  $3\pi$ , and  $4\pi$  asymmetric BW poles and the associated branching ratios) and results (parameters for the fourth pole, the coefficient  $C$  and the values for  $W0$  and  $W3$ ) [39]. We have purposely exhibited two solutions [Nos. 1 and 2] to show that it is possible to fit the sum rules yet not obtain an acceptable value of  $C$ . The graph of  $\rho_V - \rho_A$  corresponding to solution No. 3 of Table I is displayed in Fig. 13. The overall appearance of this curve clearly mimics the one in Fig. 11 which is based on the numerical approach. We view the fact that the different methods generate rather similar spectral func-

TABLE I. Asymmetric Breit-Wigner representation. The energy unit is GeV.

Trial	No. 1	No. 2	No. 3
Two-pion inputs			
$M_1$	0.763	0.763	0.763
$f_1$	0.157	0.157	0.157
$\Gamma_1$	0.123	0.123	0.123
$s_1$	$4m_\pi^2$	$4m_\pi^2$	$4m_\pi^2$
$B_{2\pi}$	0.243	0.243	0.243
Three-pion inputs			
$M_2$	1.117	1.117	1.117
$f_2$	0.244	0.234	0.250
$\Gamma_2$	0.470	0.470	0.470
$s_2$	0.500	0.510	0.550
$B_{3\pi}$	0.185	0.168	0.176
Four-pion inputs			
$M_3$	1.500	1.500	1.490
$f_3$	0.192	0.188	0.215
$\Gamma_3$	0.564	0.700	0.765
$s_3$	0.700	0.710	0.690
$B_{4\pi}$	0.048	0.041	0.053
Output values			
$M_4$	2.288	2.055	1.869
$f_4$	0.068	0.083	0.116
$\Gamma_4$	0.221	0.750	0.873
$B_{n>4\pi}$	0.0001	0.0015	0.0046
$W0$	0.0261	0.0266	0.0268
$W3$	-0.0062	-0.0062	-0.0062
$C$	0.013	0.003	$3.8 \times 10^{-5}$

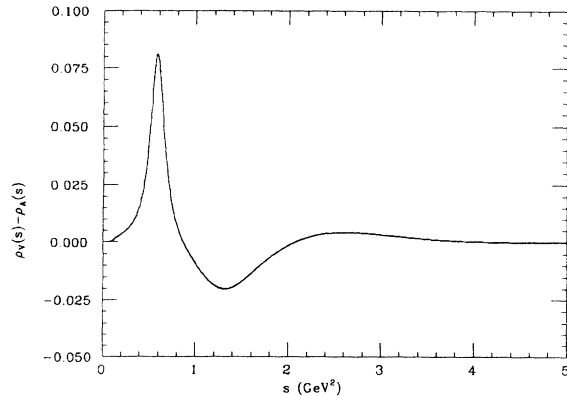


FIG. 13. Fit of asymmetric Breit-Wigner solution No. 3 to  $\rho_V - \rho_A$ .

tions as an indication that there is not great freedom in  $\rho_V - \rho_A$  once the theoretical and experimental constraints are imposed.

## VI. CONCLUDING REMARKS

What we have done in this paper is to suggest a procedure for comparing four well-known sum rules of chiral symmetry with data from the real world of experiment. In addition, we have phenomenologically constructed the vector and axial-vector spectral functions to the extent possible by using the full collection of available  $\tau$  decay and  $e^+e^-$  cross-section data. To be specific, the data which constrains the spectral functions includes the  $e^+e^- \rightarrow \pi^+\pi^-$ ,  $2\pi^+2\pi^-$ , and  $\pi^+\pi^-2\pi^0$  cross sections, the  $\tau \rightarrow 2\pi$ ,  $3\pi$ , and  $4\pi$  branching ratios, and the energy spectra for  $\pi^-\pi^0$ ,  $2\pi^-\pi^+$ , and  $2\pi^-\pi^+\pi^0$  final states in  $\tau$  decay. Theoretical constraints include chiral symmetry at low energy, isospin relations for handling the data, and the operator product expansion of QCD at high energy. It is clear to us that this activity will be repeated by ourselves or by others in the future. That is, we (perhaps optimistically) anticipate the emergence of improved data which will provide a yet more reliable foundation upon

which to base the phenomenology. However, we feel that our results are the best determination of the spectral functions that can be made at this time.

As regards the data, we urge that efforts be made to improve the determinations of the  $3\pi$  and  $4\pi$  contributions to the spectral functions. The  $3\pi$  component can only be inferred from the  $\tau$  decay hadronic distribution. In this paper, we were fortunate to have access to the recent ARGUS determination of  $\rho_A^{3\pi}$ . Cross checks are always welcome, so we urge that data from  $\tau$  production at both LEP and the Cornell Electron Storage Ring CESR be analyzed to extract the spectral function  $\rho_A^{3\pi}$ . In addition, the need for an improved  $4\pi$  determination in  $e^+e^-$  cross-section data is especially acute for the  $\pi^+\pi^-2\pi^0$  final state. Additional information on the  $4\pi$   $\tau$  decay modes ( $\pi^+\pi^02\pi^-$  or  $\pi^-3\pi^0$ ) would also be welcome.

In the latter part of our paper, we addressed the question of whether experimental data is consistent with the chiral sum rules. On the basis of our study, we conclude that existing data is indeed consistent with the chiral sum rules. It is important to not misinterpret this remark. Of course, since physical data will always be less than perfect, it is not possible to claim “proof” of validity for the set of sum rules. It is evident to us that to insist on such proof would be foolhardy. However, given the number of constraints on the spectral functions, it is far from trivial that all of the chiral sum rules can be satisfied. Agreement at the level we obtained is an affirmation of the subtle and complex theoretical intuition (involving chiral symmetry, dispersion relations, the operator product expansion, and the asymptotic behavior of QCD) that leads to the sum rules.

## ACKNOWLEDGMENTS

The research described in this paper was supported in part by the National Science Foundation. We wish to thank K. K. Gan, J. J. Gomez, F. Le Diberder, and B. Spaan for helpful correspondence and/or discussions regarding experimental aspects of spectral function determinations. We also thank A. Pérez and A. Pich for useful observations.

- 
- [1] We adopt the normalization of currents and decay constants appearing in J. F. Donoghue, E. Golowich, and B. R. Holstein, *Dynamics of the Standard Model* (Cambridge University Press, Cambridge, England, 1992).
  - [2] We work with *covariantly* defined  $T$  products.
  - [3] There turns out to be another sum rule of physical interest, related to the chiral limit of  $K$ -to- $\pi$  matrix elements of a  $\Delta S=1$  nonleptonic operator. This will be described in a separate publication.
  - [4] T. Das, V. Mathur, and S. Okubo, *Phys. Rev. Lett.* **19**, 859 (1967); J. Gasser and H. Leutwyler, *Nucl. Phys.* **B250**, 465 (1985); G. Ecker, J. Gasser, A. Pich, and E. de Rafael, *ibid.* **321**, 311 (1989).
  - [5] S. Weinberg, *Phys. Rev. Lett.* **18**, 507 (1967).
  - [6] For a study of the Weinberg sum rules following the appearance of QCD as a theory of the strong interactions, see E. Floratos, S. Narison, and E. de Rafael, *Nucl. Phys.* **B155**, 115 (1979).
  - [7] T. Das, G. S. Guralnik, V. S. Mathur, F. E. Low, and J. E. Young, *Phys. Rev. Lett.* **18**, 759 (1967).
  - [8] For example, F. Le Diberder and A. Pich, *Phys. Lett. B* **289**, 165 (1992); E. Braaten, S. Narison, and A. Pich, *Nucl. Phys.* **B373**, 581 (1992). Earlier references appear in these papers.
  - [9] Y. S. Tsai, *Phys. Rev. D* **4**, 2821 (1971). One should take care to distinguish between two commonly defined sets of spectral functions:  $v=4\pi\rho_V$  and  $a=4\pi\rho_A$ . In this paper, we work exclusively with  $\rho_{V,A}$ .
  - [10] Particle Data Group, K. Hikasa *et al.*, *Phys. Rev. D* **45**, S1 (1992).
  - [11] ARGUS Collaboration, *Z. Phys. C* **33**, 7 (1986).
  - [12] K. K. Gan, in *Proceedings of the XXVth International Conference on High Energy Physics*, edited by James R. Sanford, AIP Conf. Proc. No. 272 (AIP, New York, 1993),

- p. 427.
- [13] K. Riles, *Int. J. Mod. Phys. A* **7**, 7647 (1992).
- [14] B. C. Barish and R. Stroynowski, *Phys. Rep.* **157**, 1 (1988).
- [15] F. Le Diberder, in *Proceedings of the Second Workshop on Tau Lepton Physics*, Columbus, Ohio, 1992, edited by K. K. Gan (World Scientific, Singapore, 1992).
- [16] B. Spaan, in *Proceedings of the Second Workshop on Tau Lepton Physics* [15].
- [17] M. Davier, in *Proceedings of the Second Workshop on Tau Lepton Physics* [15]; see also Lab. de l'Accel. Lin. Report No. LAL 92-74, 1992 (unpublished).
- [18] B. H. Wiik and G. Wolf, *Electron-Positron Interactions* (Springer, Berlin, 1979).
- [19] C. Bacci *et al.*, *Phys. Lett.* **95B**, 139 (1980); *Nucl. Phys.* **B184**, 39 (1981).
- [20] D. Bisello, *The Hadron Mass Spectrum*, Proceedings of the Conference, St. Goar, Germany, 1990, edited by E. Klempt and K. Peters [*Nucl. Phys. B (Proc. Suppl.)* **21**, 111 (1991)].
- [21] Z.-P. Zheng, in *Proceedings of the 25th International Conference on High Energy Physics*, edited by K. K. Phua and Y. Yamaguchi (World Scientific, Singapore, 1991), p. 49.
- [22] V. Sidorov, in *Proceedings of the 1979 International Symposium on Lepton and Photon Interactions*, edited by T. Kirk and H. Abarbanel (Fermilab, Batavia, 1980), p. 490.
- [23] L. M. Barkov *et al.*, *Nucl. Phys.* **B256**, 365 (1985).
- [24] L. M. Kurdadze *et al.*, *Pis'ma Zh. Eksp. Teor. Fiz.* **43**, 497 (1986) [*JETP Lett.* **43**, 643 (1986)].
- [25] L. M. Kurdadze *et al.*, *Pis'ma Zh. Eksp. Teor. Fiz.* **47**, 432 (1988) [*JETP Lett.* **47**, 512 (1988)].
- [26] L. M. Barkov *et al.*, *Yad. Fiz.* **47**, 393 (1988) [*Sov. J. Nucl. Phys.* **47**, 248 (1988)].
- [27] L. Rolandi, in *Proceedings of the XXVth International Conference on High Energy Physics* [12], p. 56.
- [28] CLEO II Collaboration, *Phys. Rev. Lett.* **69**, 3610 (1992).
- [29] Mark II Collaboration, *Phys. Rev. Lett.* **56**, 812 (1986).
- [30] K. K. Gan, *Phys. Rev. D* **37**, 3334 (1988).
- [31] F. J. Gilman and S. H. Rhie, *Phys. Rev.* **31**, 1066 (1985); See also F. J. Gilman and D. H. Miller, *ibid.* **17**, 1846 (1978).
- [32] ARGUS Collaboration, H. Albrecht *et al.*, *Z. Phys. C* **58**, 61 (1993).
- [33] ARGUS Collaboration, H. Albrecht *et al.*, *Phys. Lett. B* **185**, 223 (1987).
- [34] M. A. Shifman, A. I. Vainshtein, and V. I. Zakharov, *Nucl. Phys.* **B147**, 385 (1979).
- [35] L. V. Lanin, V. P. Spiridonov, and K. G. Chetyrkin, *Yad. Fiz.* **44**, 1372 (1986) [*Sov. J. Nucl. Phys.* **44**, 892 (1986)].
- [36] J. Gasser and H. Leutwyler, *Ann. Phys. B* **158**, 142 (1984); *Nucl. Phys.* **B250**, 465 (1985).
- [37] R. D. Peccei and J. Solà, *Nucl. Phys.* **B281**, 1 (1987).
- [38] M. E. Peskin and T. Takeuchi, *Phys. Rev. D* **46**, 381 (1992); see also *Phys. Rev. Lett.* **65**, 964 (1990).
- [39] For completeness, the  $\tau$  lepton branching ratio for all  $n\pi$  modes with  $n > 4$  is also included. Although the simplicity of our description precludes taking such values too literally, the results are seen to be reassuringly small.